Journal Name

RSCPublishing

ARTICLE

Laser direct-write for fabrication of three-dimensional paper-based devices

Cite this: DOI: 10.1039/x0xx00000x

P. J. W. He, I. N. Katis, R. W. Eason and C. L. Sones

Received 00th January 2012,
Accepted 00th January 2012

DOI: 10.1039/x0xx00000x

www.rsc.org/

We report the use of a laser-based direct-write (LDW) technique that allows the design and fabrication of three-dimensional (3D) structures within a paper substrate that enables implementation of multi-step analytical assays via a 3D protocol. The technique is based on laser-induced photo-polymerisation, and through adjustment of the laser writing parameters such as the laser power and scan speed we can control the depths of hydrophobic barriers that are formed within a substrate which, when carefully designed and integrated, produce 3D flow paths. So far, we have successfully used this depth-variable patterning protocol for stacking and sealing of multi-layer substrates, for assembly of backing layers for two-dimensional (2D) lateral flow devices and finally for fabrication of 3D devices. Since the 3D flow paths can also be formed via a single laser-writing process by controlling the patterning parameters, this is a distinct improvement over other methods that require multiple complicated and repetitive assembly procedures. This technique is therefore suitable for cheap, rapid and large-scale fabrication of 3D paper-based microfluidic devices.

Introduction

Paper-based microfluidic devices have drawn considerable attention over the last few years, as they possess many intrinsic advantages such as low-cost, capability of mass production, and are disposable, equipment free, and require no external power to operate.[1-4] However, there are also some disadvantages and limitations, such as issues with the control of flow rate, multiplexed detection of assays on a single device and there is a constant drive to further reduce the size in order to achieve compact devices that require a smaller volume of reagents with shorter fluid distribution times.[5-7] As a result, 3D microfluidic paper analytical devices, which enable fluid distribution in both lateral and vertical directions, have also been proposed in recent years.[4, 8-10]

Compared with a conventional 2D geometry, 3D devices provide a number of unique characteristics which are advantageous for certain applications.[11] As an example, in the case of a multi-layered 3D device, which is a stack of substrates that can be of dissimilar materials, fluid-flow can be in all three dimensions, i.e. both laterally in the plane of any substrate layer, and vertically through the thickness of all layers that form the composite, and such devices would thus enable a user to perform several assays within the same device footprint.[8] When compared to a lateral flow device (LFD), such flow-through geometries provide flow paths that are comparatively shorter and therefore provide the capability for implementation of multiple-step assays via more compact device geometries.[8] Additionally, such compact 3D devices can minimise the quantity of reagents that are either required or wasted, in the case of 2D devices, as a result of soaking of the greater lengths and volumes of the porous substrates. Lastly, shorter flow paths obviously translate into a reduced fluid distribution or delivery time leading to likely reductions in times for operation of such tests.[11]

So far, for almost all of the reports in the literature, 3D paper-based microfluidic devices have been fabricated by sequential assembly of individual layers of 2D devices. Therefore, in addition to the critical requirement for correct alignment of individual layers, another key challenge encountered in the fabrication of such 3D devices is ensuring sufficient contact between the hydrophilic sections of each layer that constitute the flow-path because any lack of contact will result in an interrupted flow-path.[7] Three general solutions have been reported for avoiding this problem, which include: 1) forming the structure in a layer-by-layer manner with use of either double-sided tape or a hydrophilic spray adhesive;[8, 11] 2) applying an outer adhesive, clamp, or protective coating to pre-assembled layers thus holding the layers in contact with each other;[9, 12] and, 3) by forming 3D structures in a single layer of paper substrate which therefore circumvents this problem completely.[13]

3D paper-based microfluidic devices were first reported by the Whitesides` group who used double-sided tape to physically attach individual 2D devices together, which had been pre-

patterned using a photolithographic method.[8] At places where the desired flow through is required, laser-drilled holes were created in the tape and filled with cellulose powder in order to create hydrophilic connections between the adjacent layers of paper. However, this method is somewhat labour-intensive as there are several sequential assembly processes that must be accomplished and hence it does not readily lend itself to mass fabrication. An alternative technique reported the use of hydrophilic spray adhesive to glue layers of pre-patterned 2D devices together, which then allows more rapid laboratory-based fabrication of 3D devices.[11] As this method relies on cold lamination techniques to hold and seal together layers of stacked 2D devices, it is only able to produce 3D devices that incorporate two or three layers of paper, and so is not practicable for devices requiring more layers.[14, 15] Subsequent work by Crooks et al. reported an alternative method for creation of 3D paper-based devices based on the principle of origami, the traditional Japanese paper-folding art.[9, 12, 13] In this approach, a 3D device is achieved by laying and folding a single piece of pre-patterned paper and then the stack is held together via a clamp. The origami technique allows patterning of different layers of paper in one go and additionally eliminates complex alignment steps. Such a folded design also enables opening and altering the device during the reagent preparation step and even during the course of an assay.[13, 16] However, this method can cause issues of reproducibility as it relies on the individual performing the test following the instructions given and there is then the possibility of an incorrect procedure occurring, particularly if the person is performing the assembly for the first time. Overall, most of these reported methods were based on fabrication of 3D devices using cellulose paper. However, other porous materials, such as threads,[17, 18] cloth,[19] and silk fabric,[20] have also been explored by different groups for fabrication of 3D microfluidic devices.

Unlike all the methods discussed above, in this article, we report a new approach for the fabrication of 3D devices, which is a simple extension of the basic LDW technique that has been described in our previous publications for both fabrication of 2D microfluidic devices and implementation of flow-control.[21-23] In brief, by controlling the laser patterning conditions, we have shown that we can produce solid hydrophobic structures either partially inside a single layer of paper or all the way through several layers of paper (we have so far demonstrated 3 separate layers). Also, by selectively patterning from both sides of the composite substrate, we have fabricated 3D devices based on both a single layer as well as a multi-layer stacked arrangement. Unlike other 3D device fabrication methods, the approach presented here does not require any additional processing equipment, alignment or assembly steps and, as described earlier, uses the same proven fabrication approach that we have demonstrated for 2D fluidic flow path devices.

Experimental Section

Laser setup and materials

The laser used for the LDW process was a 405 nm continuous wave diode laser (MLD^{TM} 405 nm, Cobolt AB, Sweden) with a maximum output power of ~110 mW). The basic LDW setup is the same as described in our previous publications for fabrication of 2D microfluidic devices and implementation of flow-control and has been fully optimised via a series of systematic studies.[21-23] The results we have achieved and will report in the following sections are therefore based on the same patterning procedure with appropriate adjustment of the patterning conditions such as laser power and scan speed.

The paper substrates used were Whatman® No. 1 filter paper and Polyvinylidene fluoride (PVDF) from GE Healthcare Inc., UK was used for realizing stacking and sealing. Ahlstrom® Grade 320 and 222 chromatography paper from Ahlstrom, Finland, were used for fabrication of backing and 3D structures described below. The photopolymer chosen for these experiments was Sub G, from Maker Juice, USA. The solvent used in development step was Acetone from Sigma Aldrich Co Ltd., UK. The inks used for validating our patterned devices were blue and red bottled inks from Parker, UK.

Results and discussion

Stacking and sealing of multi-layer papers

During our earlier LDW studies for fabrication of 2D paper-based microfluidic devices, we observed that the photo-polymerization process is not restricted to a single substrate but can also extend further into a composite formed from several layers. In order to understand and further explore this phenomenon, we prepared samples with different numbers of layers (two to five) and investigated their patterning using the same LDW method. The schematic for this is shown in Figure 1: firstly, different numbers of cellulose papers were stacked together and then soaked with the photopolymer. The same LDW patterning process was applied to form simple structures in these multi-layered samples. After the final development process, it was then observed that these multi-layers had been efficiently bonded together to form a single composite structure.

Based on our current setup with a 405 nm c.w. laser, we found that a maximum of three layers of cellulose paper (each with thickness of 180 µm) can be bonded together using a laser output power of 100 mW at a scan speed of 10 mm/s. The polymerised lines were evident throughout all three layers of paper and as shown in Figures 2a and 2b, can be clearly observed on both sides of the three-layer stack. We then tested these structures by applying different volumes of blue ink, from 3 µL to 7 µL, into these square wells from the top surface as shown in Figure 2c. The ink was well-confined within the square wells defined by the polymerised walls and flowed vertically from the upper layer to the layers underneath. The result is shown in Figure 2d: 3 µL of blue ink is just enough to reach the third layer, while the whole square well of all three layers get fully inked with a volume of 6 µL while 7 µL is seen

to produce slight overflowing. It is clear therefore that the polymerised structures that extend from the top layer all the way to the bottom layer perform the dual function of bonding and forming walls that contain and hold the fluid without any leakage, as seen for the image using 6 µL in figure 2d.

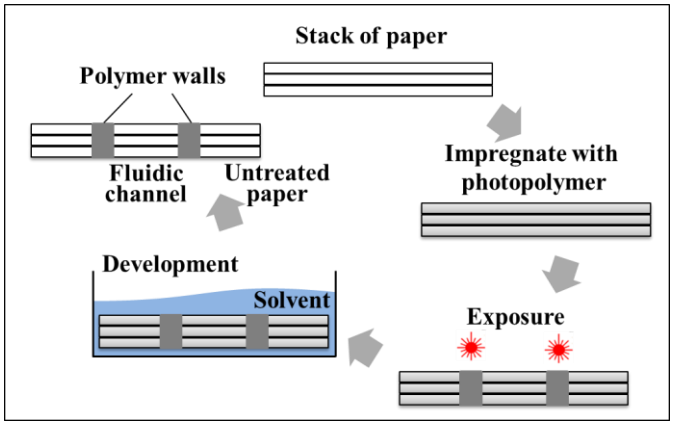

Figure 1 Schematic of patterning multi-layer stacks using the LDW technique.

Using the same parameters, we then attempted to pattern stacks with four layers but although the layers were indeed bonded together, leakage was much more of an issue, so under our normal patterning process conditions, we did not pursue composites with greater than three layers. However, stacked structures with more layers would indeed be possible through choosing different patterning parameters, such as lower scan speed and higher incident power.

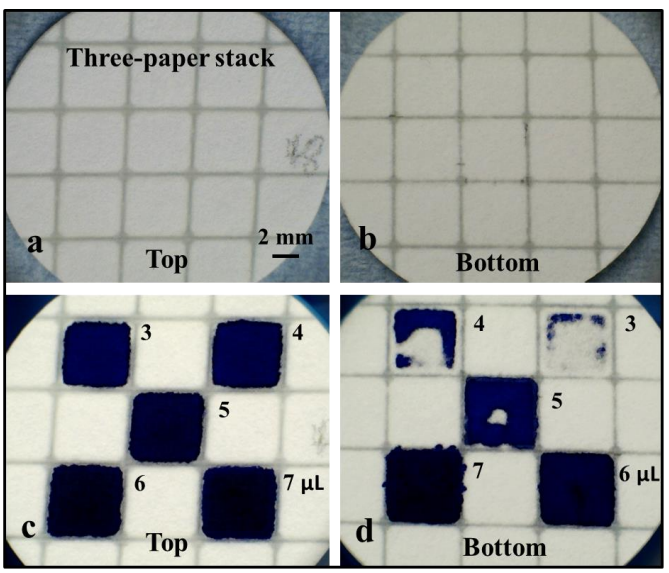

Figure 2 Images showing the polymerised structures from both sides a) top side, b) bottom side) of a stack with three layers of cellulose paper and images of both sides of the device c) top side, d) bottom side) after introduction of blue ink of different volumes (3-7 µL) into the designated well.

Following these first trials we then trialled assembly of multi-layer stacks but this time composed of dissimilar substrate materials. The schematic image in Figure 3a shows our first realisation of a stacked structure using different materials: two layers of cellulose paper with a PVDF layer in between that have been bonded together via a common photo-polymerization process. The rectangular channel and a T-junction shown in the schematic were patterned on the top and bottom surface respectively with a laser power of 50 mW at a scan speed of 10 mm/s. The four sealing points which extend throughout all of the three layers and enable their bonding were formed by illuminating each point with a stationary laser beam (100 mW) for 5 seconds. To test the device, red and blue inks were separately introduced onto the top and the bottom surfaces of this stack, and as shown in Figure 3b and 3c the inks were guided in the channel and T- junction respectively. From Figure 3b and 3c it can also be clearly observed that both inks flow only within their respective layers and did not penetrate through to the opposite layer, due to the presence of the intermediate blocking layer (hydrophobic PVDF). This innovative result presents a solution for not only sealing of paper-based devices by isolating the device between dissimilar outer cladding layers but also, most importantly, permitting 3D pathways to be engineered through judicious assembly of several layers, possibly combined with holes and voids in some layers. In our earlier publications using the same laser-direct write technique,[21, 22] we have demonstrated the patterning of varied porous materials such as nitrocellulose membranes, printing paper, fabrics, and we therefore believe that any such material which is porous in nature would be suited for use in the production of the above described multi-layer devices. There are no other requirements that we believe would limit the use of a specific type of material for the creation of multi-layered devices.

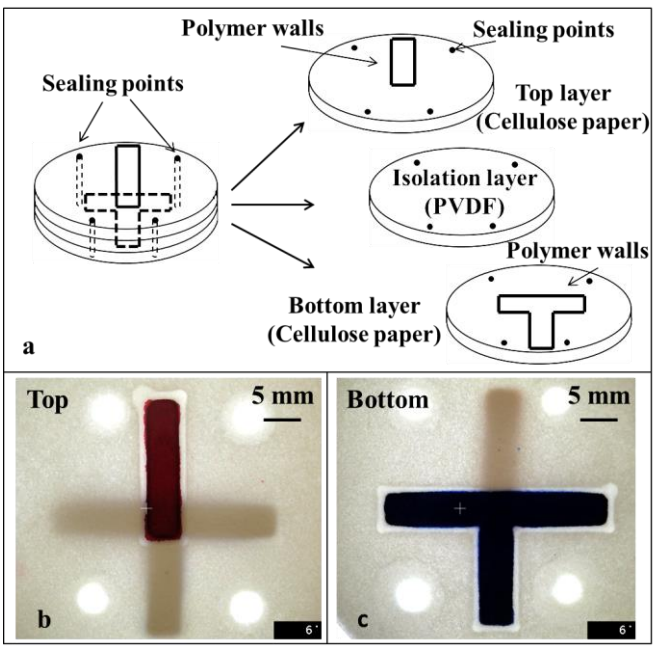

Figure 3 a) Schematic image showing the arrangement of a stacked device with different structures in top and bottom layers, which are isolated with a hydrophobic film in between. b) Top and c) bottom images showing the device described in a) after the introduction of different inks from top and bottom surfaces without any cross-contamination or mixing.

Any paper-based device is normally intended for operation under ambient conditions, which can lead to a number of limitations when compared to fully enclosed microfluidic devices. Two of the main drawbacks are: a) the device is at risk of contamination during the fabrication, transportation and operation, and b) possible evaporation of the fluid in the open air which may lead to change of the sample concentration, or an altered flow rate due to change in sample viscosity.[24, 25] We believe that the results we have achieved above should contribute to a reduction of these two limitations by sandwiching a conventional paper-based microfluidic device with two outer layers of hydrophobic material. The LDW technique can be further extended to develop a new approach that helps with sealing in microfluidic paper-based analytical devices (μPAD). Additionally, the technique could also be further employed for permitting 3D pathways through carefully designing the patterning protocol and subsequent assembly of several layers for realisation of a practical 3D paper-based device.

Single-sided polymerisation – for backing a paper-based device

To our knowledge, all or most of the presently reported paper-based microfluidic devices have another important limitation - operation of these unbacked devices require that their bottom faces remain isolated from contact with any surface to prevent fluid flow along the interface which would provide an alternative undesirable flow path. In addition to the loss of the fluid (an expensive reagent or valuable sample present in small volumes for example) this unwanted flow can also lead to cross-contamination which in turn may produce a false result or failed test.[24] On the other hand, as paper is normally very fragile and more so especially after getting wet, a backing support to provide mechanical strength would normally be desirable. For the case of nitrocellulose (NC) membrane-based devices, the support to the membrane can be provided by an impermeable polyester layer.[26] While it is easy to procure such pre-backed NC membranes which are extensively used in LFD, it is not yet possible to source similar backed versions of paper substrates from the market. As an alternative, tape is widely used to back paper-based devices,[26] but this has certain drawbacks as the adhesion becomes poor when the paper gets wet following the introduction of the sample; additionally, the adhesives in tapes can diffuse into paper over time, which can lead to contamination as well as affecting the paper`s hydrophilicity.[24] Another method of backing paper-based devices is based on flexography printing: a thin layer of polystyrene is printed on one side of the paper to form a hydrophobic backing,[27] but this method requires additional equipment and adds cost to the final devices.

We therefore introduce here the use of our LDW technique as a new solution for backing paper-based devices. From the experiments we have done previously, we have observed that by controlling the patterning parameters, (laser incident power and scan speed), we could alter the depth of polymerised structures inside the substrate which thereby forms a hydrophobic polymerised layer within the substrate itself, which could be used as the backing layer. Compared with the methods currently used for backing, our LDW method allows formation of a backing structure inside the substrate during the device fabrication procedure without any need for extra materials or equipment, which would then lead to cost reduction and simplicity of fabrication. The schematic illustrating this is shown in Figure 4: the paper substrate is first impregnated with photopolymer, then during the exposure step the laser parameters are selected to polymerise only to a certain depth inside the substrate. After the final development process, the un-polymerised material is washed away, leaving behind a polymer layer with a specified depth inside the substrate, which thereby serves as the required backing.

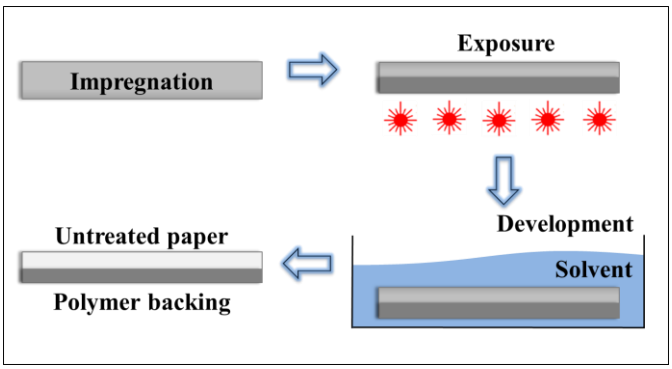

Figure 4 Schematic of patterning a backing layer inside the paper substrate using the LDW technique.

We therefore performed a parametric study to understand the influence of different patterning parameters, which also included a number of repetitive scans. The basic LDW setup is the same as described previously and the paper substrates used were Ahlstrom® Grade 320 chromatography paper with a thickness of 2.48 mm. As a proof-of-principle, in order to form a backing structure, we scanned the laser beam across the substrate in a line-by-line manner with a centre-to-centre separation of 1 mm (as shown in Figure 5a), which was appropriate for the lines to just touch each other without any significant overlap or gaps. By forming adjacent polymerised lines under the same writing conditions, it was possible to create a 2D polymerised layer inside the substrate.

The cross-sectional images in Figure 5b and 5c show examples of a patterned paper with different thicknesses of polymerised layers formed at the bottom of the substrate that was achieved by simply altering the patterning parameters. As shown in Figure 5b and 5c, after introducing red ink from the un-polymerised side, we could clearly identify the polymerised

layers (white region). As seen in the images: the thickness of the polymerised structures increases from ~ 700 µm to ~ 1 mm with an increase of laser output power from 30 mW to 70 mW at a fixed scan speed of 5 mm/s. As shown in both images, the polymerised layer, although written in a line-by-line manner was continuous and uniformly thick, and the demarcating interface between the un-polymerised and polymerised section is clearly defined.

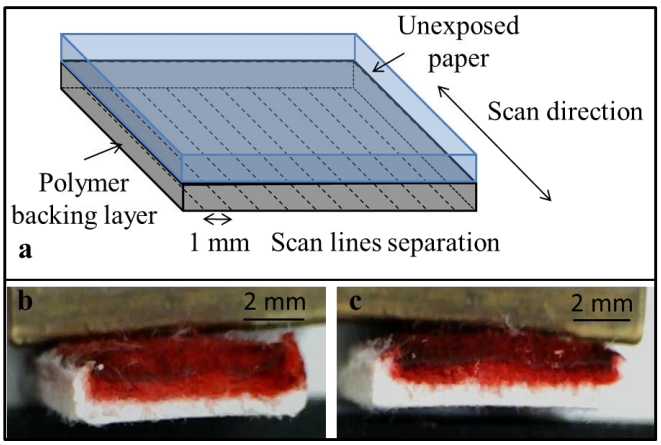

Figure 5 a) Schematic of patterning a backing structure by scanning the laser beam across the substrate in a line-by-line manner with a separation of 1 mm. Cross-section images showing polymerised layers (un-inked white layers) on one side of thick cotton fibre filter paper with different thickness of: b) ~ 700 µm and c) ~ 1 mm, after introduction of red ink from the other side.

To further study the depth of the polymerised layers as a function of the patterning parameters, we performed a study with the results shown in Figure 6. For a fixed scan speed, as expected, the depth of the polymerised layer increases with an increase of the incident laser power. For example, at a fixed scan speed of 10 mm/s, the depth of the polymerised layer increases from ~400 µm to ~950 µm with an increase of laser output power from 10 mW to 100 mW. Similar behaviour was observed with a layer depth increase from ~ 450 µm to ~ 1050 µm and ~ 1200 µm to ~ 2050 µm at a fixed scan speed of 5 mm/s and 1 mm/s respectively for incident laser power ranging from 10 mW to 100 mW. As expected, we can also observe from the same plots that the depth of the polymerised layers increases with the decrease of the scan speed at fixed laser powers.

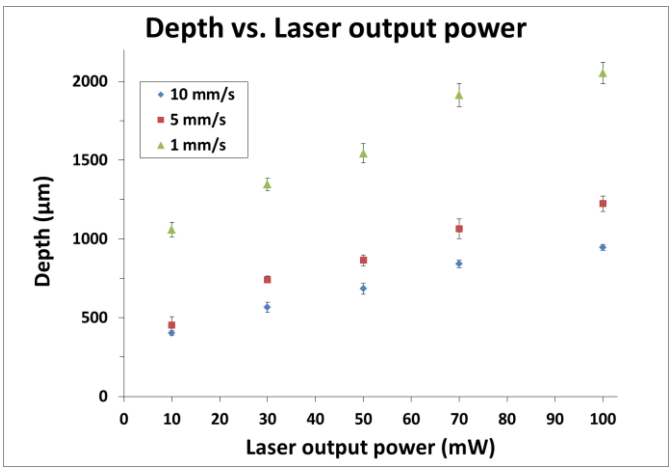

Figure 6 Plots showing the variation in the depth of the polymerised layers for different laser powers at three different scan speeds. Error bars indicate the standard deviation for 5 measurements.

Additionally, we observed that the depth of a single polymerised line also depends on the number of scans performed under the same writing conditions, which thereby alters the resulting thickness of the polymerised backing layers. In order to study how the number of scans affects the polymerised depth, we scanned the beam once, twice and three times respectively under the same writing conditions. The histogram in Figure 7 shows that the depth of the polymerised layer increases monotonically with an increasing number of repeat scans. As shown in the plots, the depth of the polymerised layer increases from ~ 400 µm to ~800 µm with an increase of the number of scans from one to three at a patterning condition of 10 mW of incident power at 10 mm/s scan speed. Similar trends were observed for all laser powers used (30, 50, 70 and 100 mW) for the same scan speed of 10 mm/s.

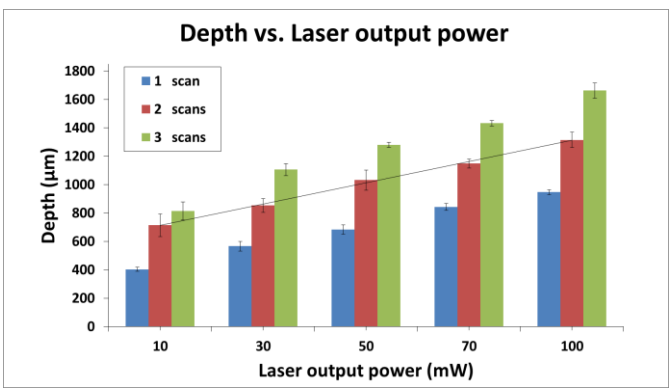

Figure 7 Plots showing the variations in the depths of the polymerised layers for different laser powers at a fixed scan speed of 10 mm/s for three different numbers of scans. Error bars indicate the standard deviation for 5 measurements and a linear line for the case of 2 scans is a simple guide for the eye.

Single-sided polymerisation – for reduction in the dead-volume of a paper-based device

An additional benefit of this technique lies in the reduction of the active paper volume that can be produced routinely for all such test substrates, which leads to a corresponding reduction of reagent/sample volume required. Due to the opacity of the substrate, the observable signals (the colour change) that provide the test results originate only from the top region or plane of the substrate (which for a nitrocellulose membrane extends below the surface to a depth of ~10 µm), and any colour change from deeper regions (the so-called dead volume) makes a negligible contribution to the observable signal, and is therefore redundant.[28] Reduction of the thickness of the substrate at the detection area will therefore not only help with saving of reagent/sample but will also help increase the limit of detection. Because the amount of the sample which previously would have soaked the entire volume of the substrate will now instead fill up a comparatively smaller volume of the substrate, the sample concentration will be relatively higher and thus will lead to an improved limit of detection.

To test this hypothesis, as shown in Figure 8a, a simple proof-of-principle experiment was performed by introducing different volumes (1, 2 and 3 µL) of red ink into 4 × 5 mm well structures patterned on samples 1 and 2, which were backed with layers that had different thickness of ~400 µm and ~600 µm, using the LDW method. These backing layers were first formed by scanning the laser in a line-by-line format using laser powers of 10 mW and 40 mW respectively at a scan speed of 10 mm/s. The line-patterns of the grid-structures were patterned by scanning the laser once along the paper surface with a power of 20 mW at a scan speed of 10 mm/s. The paper substrates used for both samples were Ahlstrom® Grade 222 chromatography paper with a thickness of 0.83 mm. As shown in Figure 8a, the colour intensities change in each well with different ink volumes and also differ between the two samples with different thickness of backing for the same volume. The images were processed with the ImageJ software (National Institutes of Health, USA) to extract the respective grayscale colour intensities of the red colour produced within the central area of each well and the results are plotted in Figure 8b. The conclusion here is that the detected colour intensity increases with an increase of the ink volume, but more importantly, also increases with an increase of the backing thickness, i.e. the signal is enhanced with a reduction of the dead volume. We therefore believe that by designing and choosing the appropriate thickness of the backing, we should be able to control the volume of substrate and hence reduce the dead volume thereby increasing the sensitivity and saving on sample or reagent needed.

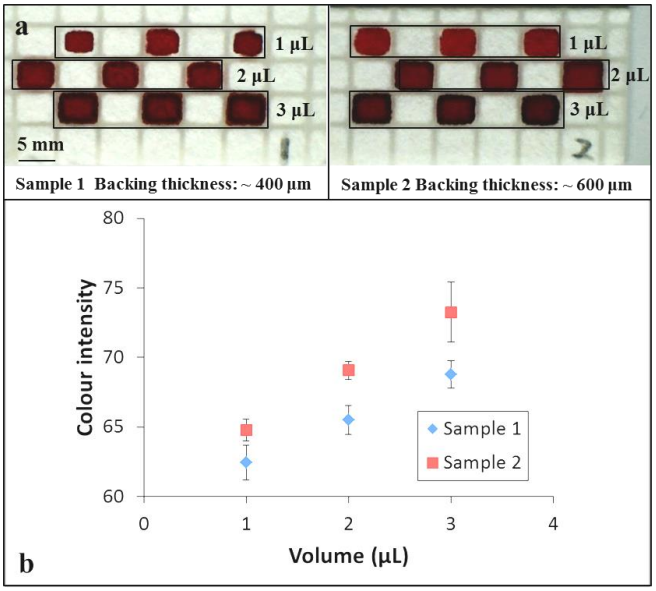

Figure 8 (a) Images showing the results of introduction of different volumes of red ink into 4 × 5mm well structures patterned in two samples with different backing thickness. (b) Plots constructed using the grayscale intensity values taken from the images shown in (a). Error bars indicate the standard deviation for 3 measurements.

In summary, we have proved that by simply changing the patterning parameters, we can polymerise lines with different depths in the substrate, and therefore, by scanning lines in a line-by-line manner we could form polymerised layers with the desired depths, and these can be used either as backing for paper-based devices or to alter the volume of the paper-based fluidic device. Here, for our first simple proof-of-principle experiment, we have used an un-optimised line-by-line scanning procedure in order to cover a large area. Alternatively, instead of repetitive multiple scanning protocols, a single-step process that uses a cylindrical lens could also be employed. In this case the lens focuses the beam only in one direction and leaves the other direction wide enough to cover an extended lateral region and this is an intended future approach.

Dual-sided polymerisation – for fabrication of a 3D paper-based device

In order to exploit fully the true potential of this approach we have explored the possibility of creating such polymerised patterns though exposure from either side of a single substrate. The objective here was to use this dual-sided polymerisation protocol to fabricate a 3D device in a single paper substrate. The concept is explained through the schematic depicted in Figure 9a. As shown in this figure, by patterning via exposure from both the top and bottom faces of a single paper substrate it should be possible to create polymerised blocks that extend partially from both faces of the substrate and define an enclosed flow-path that is embedded within the substrate. By selectively positioning and connecting such polymerised areas, we can

then construct arbitrarily-shaped connected 3D flow paths that guide the fluid both in the horizontal and vertical directions. The schematic in Figure 9b shows an example of such 3D paper-based devices created in a single substrate with several fully enclosed and interconnected channels. As shown in the cross-section schematic, solid polymerised barriers were formed from both top and bottom, leaving gaps in both vertical and horizontal directions. The gaps in the vertical direction form three open windows A, B and C, where the reagent/sample will appear after passing through the enclosed channels between the two inlets (①②). The enclosed channels that connect the inlets and three open windows are defined by gaps between the solid barriers in the horizontal direction. Photographic images of the top and bottom views of a real device with the illustrated arrangement are shown in Figure 9c: the white areas are bare/un-polymerised sections of paper and the pale yellow areas are the hydrophobic polymerised regions. All of the polymerised blocks shown in the schematic in Figure 9 and the devices in Figure 10 to 12, were patterned by scanning the laser in a line-by-line manner to create lines with a centre-to-centre separation of 1 mm using a laser output power of 100 mW at a scan speed of 10 mm/s. The resultant blocks had thicknesses of ~ 950 µm and hence for a substrate that had a thickness of 2.48mm, the enclosed flow-path had a height of 580 µm.

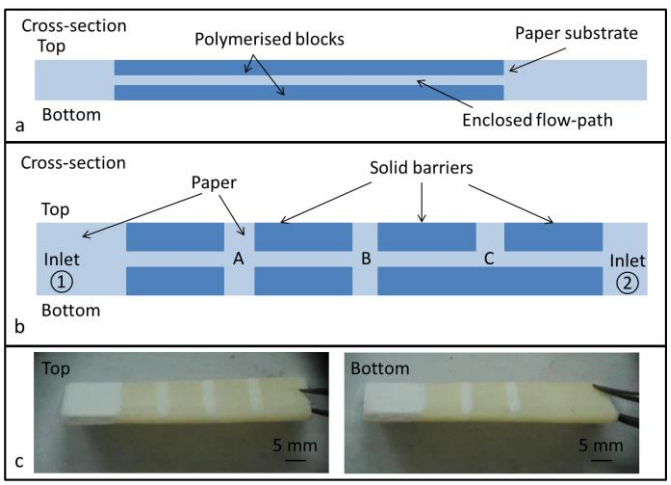

Figure 9 a) Schematic showing an enclosed flow-path formed by creating polymerised blocks from both faces of a single paper substrate. b) Schematic representation of cross-section of a 3D fluidic device with two inlets (①②) from either end. c) Photographic images taken from the top and bottom of the device described in b).

In order to test these 3D structures, we first introduced red ink from the inlet ① of the device described in Figure 9b. The sequential images in Figure 10 show the flow of red ink, which were taken from both top and bottom faces of the device. After the introduction of the ink, it flowed into the first enclosed channel between inlet ① and the open window A. The red shaded areas were observed from both sides of the device and illustrate the ink flow inside the channel. After a short period of time, the ink flowed through the first section of the enclosed channel and reached the open area A: as shown in the images the red ink has filled in the area A and is visible from both top and bottom.

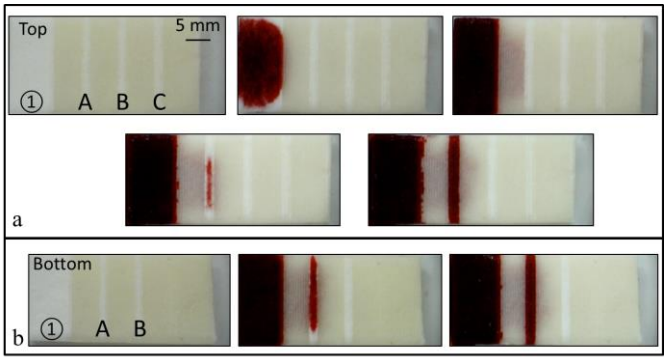

Figure 10 Sequential images taken from the a) top and b) bottom showing the device described in Figure 9b after introduction of red ink from the inlet ①.

We have also introduced red ink from the inlet ② and the result is shown in Figure 11. The ink again flowed through the enclosed channel between inlet and the open area B and finally reached the open window C and hence appeared on the top side. The difference of the structures in the right and the left sections of the device is that the polymerised structures at the bottom cover the whole area without having an open window. It can be regarded as a 3D device with an enclosed channel and an open window just on the top plus a backing structure underneath, which helps to provide support to the device.

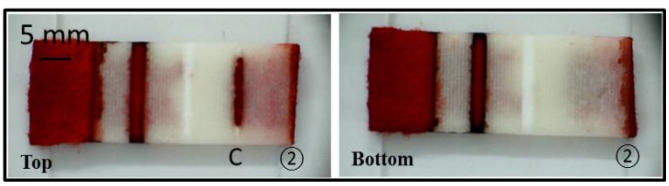

Figure 11 Photographic images showing the top and bottom of the device described in Figure 9b after introduction of red ink from the inlet ②.

Finally, the cross-section image in Figure 12 illustrates the flow process of the red ink inside this 3D device. The narrow red lines inside the substrate, which connect the inlets and open areas, show the flow of the red ink inside the enclosed channels. The ink from inlet ① flowed and filled up the open area A, which allows the ink to be seen from both top and bottom, through an enclosed channel in between and then kept flowing towards the open area B along another enclosed channel. Similarly, the ink filled in the open area C and shows up only from the top with the source from the inlet ② again through an enclosed channel inside the substrate that was formed with solid blocks on both sides. Such fully enclosed channels can be

achieved easily with our LDW method, which prevents liquid exchange between the exterior and the interior of the channel.

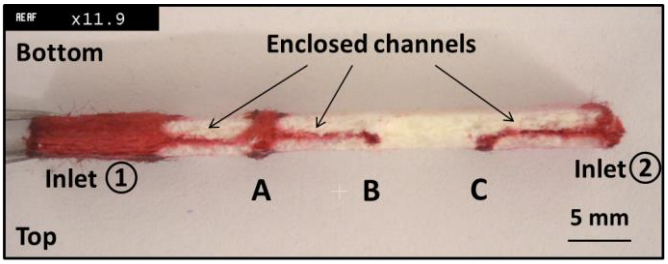

Figure 12 Cross-section image showing the enclosed channels and flow of the red ink in the device described in Figure 9b after introduction of ink from both inlets.

Above all, the approach reported here for fabrication of 3D paper-based devices is a simple extension of the basic LDW technique that has been used for fabrication of 2D microfluidic devices.[21, 22] Through selectively designing and patterning polymerised structures from both sides of the substrate, we could fabricate 3D structures inside a single substrate. Unlike other 3D device fabrication methods, the approach presented here does not require any additional processing equipment or alignment/assembling step and uses the same fabrication approach described earlier for producing a 2D fluidic device.

Conclusions

In summary, we have proposed and demonstrated a novel method, which can be used for stacking and sealing, fabrication of backing structures and construction of 3D structures in paper or porous substrates. The method is based on the same LDW technique we have reported previously with simple modification of the patterning parameters during the fabrication procedure, so that the polymerization process can extend through a few layers of substrate that are stacked together. This can be used for sealing the devices in order to solve potential evaporation and contamination problems. By simply changing the patterning parameters, a polymer backing layer with a specific thickness can be patterned within the paper substrate itself, which can be used as backing for paper-based devices instead of the currently used tape or polyester film. In addition, the thickness of this polymerised layer can be controlled to reduce the paper volume, which in turn allows reduction of the required reagent/sample volume and most importantly, can be used to increase the limit of detection.

Finally, we showed the possibility of fabrication of 3D paper-based devices as the polymerised structure can be formed inside the substrate with a controllable thickness. As a result, through selectively designing and patterning some of these polymerised structures from both sides of the substrate, we could fabricate 3D structures inside a single layer of substrate. Unlike other 3D device fabrication methods, our LDW approach does not require any additional processing equipment or alignment/assembling steps and uses the same fabrication approach that is applied for producing a 2D fluidic device by simply altering the patterning parameters.

Acknowledgements

The authors acknowledge the funding received via the Engineering and Physical Sciences Research Council (EPSRC) Grant Nos. EP/J008052/1, EP/K023454/1, EP/N004388/1 and EP/M027260/1, and the funding received via a Knowledge Mobilisation Fellowship for Dr. Collin Sones from the Institute for Life Sciences and the Faculty of Health Sciences of the University of Southampton. The underpinning RDM data for this paper can be found at 10.5258/SOTON/387274.

Notes and references

[a] *Optoelectronics Research Centre, University of Southampton, Highfield, Southampton, U.K. SO17 1BJ. Tel:44 2380 599091; E-mail: ph3e12@soton.ac.uk*

1. J. L. Osborn, B. Lutz, E. Fu, P. Kauffman, D. Y. Stevens and P. Yager, *Lab Chip*, 2010, **10**, 2659-2665.
2. A. C. Siegel, S. T. Phillips, M. D. Dickey, N. S. Lu, Z. G. Suo and G. M. Whitesides, *Adv. Funct. Mater.*, 2010, **20**, 28-35.
3. K. Abe, K. Suzuki and D. Citterio, *Anal. Chem.*, 2008, **80**, 6928-6934.
4. D. Sechi, B. Greer, J. Johnson and N. Hashemi, *Anal. Chem.*, 2013, **85**, 10733-10737.
5. N. Hashemi, J. S. Erickson, J. P. Golden and F. S. Ligler, *Biomicrofluidics*, 2011, **5**, 9.
6. N. Hashemi, J. S. Erickson, J. P. Golden, K. M. Jackson and F. S. Ligler, *Biosens. Bioelectron.*, 2011, **26**, 4263-4269.
7. A. K. Yetisen, M. S. Akram and C. R. Lowe, *Lab Chip*, 2013, **13**, 2210-2251.
8. A. W. Martinez, S. T. Phillips and G. M. Whitesides, *Proc. Natl. Acad. Sci. U. S. A.*, 2008, **105**, 19606-19611.
9. H. Liu and R. M. Crooks, *J. Am. Chem. Soc.*, 2011, **133**, 17564-17566.
10. L. Ge, J. X. Yan, X. R. Song, M. Yan, S. G. Ge and J. H. Yu, *Biomaterials*, 2012, **33**, 1024-1031.
11. G. G. Lewis, M. J. DiTucci, M. S. Baker and S. T. Phillips, *Lab Chip*, 2012, **12**, 2630-2633.
12. H. Liu, Y. Xiang, Y. Lu and R. M. Crooks, *Angew. Chem.-Int. Edit.*, 2012, **51**, 6925-6928.
13. C. Renault, J. Koehne, A. J. Ricco and R. M. Crooks, *Langmuir*, 2014, **30**, 7030-7036.
14. S. J. Vella, P. Beattie, R. Cademartiri, A. Laromaine, A. W. Martinez, S. T. Phillips, K. A. Mirica and G. M. Whitesides, *Anal. Chem.*, 2012, **84**, 2883-2891.
15. N. R. Pollock, J. P. Rolland, S. Kumar, P. D. Beattie, S. Jain, F. Noubary, V. L. Wong, R. A. Pohlmann, U. S. Ryan and G. M. Whitesides, *Sci. Transl. Med.*, 2012, **4**, 10.
16. A. V. Govindarajan, S. Ramachandran, G. D. Vigil, P. Yager and K. F. Bohringer, *Lab Chip*, 2012, **12**, 174-181.
17. M. Reches, K. A. Mirica, R. Dasgupta, M. D. Dickey, M. J. Butte and G. M. Whitesides, *ACS Appl. Mater. Interfaces*, 2010, **2**, 1722-1728.
18. X. Li, J. F. Tian and W. Shen, *ACS Appl. Mater. Interfaces*, 2010, **2**, 1-6.
19. A. Nilghaz, D. H. B. Wicaksono, D. Gustiono, F. A. A. Majid, E. Supriyanto and M. R. A. Kadir, *Lab Chip*, 2012, **12**, 209-218.
20. P. Bhandari, T. Narahari and D. Dendukuri, *Lab Chip*, 2011, **11**, 2493-2499.
21. C. L. Sones, I. N. Katis, P. J. W. He, B. Mills, M. F. Namiq, P. Shardlow, M. Ibsen and R. W. Eason, *Lab Chip*, 2014, **14**, 4567-4574.
22. P. J. W. He, I. N. Katis, R. W. Eason and C. L. Sones, *Biomicrofluidics*, 2015, **9**, 10.
23. P. J. W. He, I. N. Katis, R. W. Eason and C. L. Sones, *Lab Chip*, 2015, **15**, 4054-4061.

24. K. M. Schilling, A. L. Lepore, J. A. Kurian and A. W. Martinez, *Anal. Chem.*, 2012, **84**, 1579-1585.
25. E. da Silva, M. Santhiago, F. R. de Souza, W. K. T. Coltro and L. T. Kubota, *Lab Chip*, 2015, **15**, 1651-1655.
26. E. M. Fenton, M. R. Mascarenas, G. P. Lopez and S. S. Sibbett, *ACS Appl. Mater. Interfaces*, 2009, **1**, 124-129.
27. J. Olkkonen, K. Lehtinen and T. Erho, *Anal. Chem.*, 2010, **82**, 10246-10250.
28. R. L. F. S.-c. f. p. development, *Millipore Corporation, Billerica, MA*, 9-10.